SIMPLIFIED MODELS OF PILOT BIOMECHANICS FOR ROTORCRAFT VERTICAL BOUNCE ANALYSIS

Tommaso Aresi[1], Andrea Zanoni[1], Gianni Cassoni[1] & Pierangelo Masarati[1]

[1]Dipartimento di Scienze e Tecnologie Aerospaziali, Politecnico di Milano, Milano, Italia

Abstract

Vibrations in rotorcraft result from the interaction between the rotors' mechanical components and the airflow on the blades. These vibrations can cause structural fatigue, reduce operational efficiency, and even impact operational safety by affecting pilots and operators. The phenomena where pilot biomechanics interact with vehicle vibrations, affecting flying qualities, are known as (Adverse) Rotorcraft-Pilot Couplings (RPCs). Pilot-Assisted Oscillations (PAOs) are a specific type of RPC, occurring in the 2 Hz–8 Hz range, beyond the control of human manual input, and often involve unintentional pilot inputs. For collective bounce analysis, the aircraft heave motion and collective flap dynamics are crucial for stability analysis. Pilot models range from simple linear models to detailed multibody models of the human upper body. The analysis of PAOs involves modeling and testing the BioDynamic FeedThrough (BDFT), which describes the input-output relationship in the Pilot Control Device System. The objectives of this modeling are to identify the contributions influencing BDFT, physically represent the components of the block scheme, verify results from different applications, and develop a simplified model for control synthesis.

Keywords: Pilot Biomechanics, Rotorcraft Pilot Coupling, BioDynamic FeedThrough, Pilot Assisted Oscillations, Collective Bounce

1. Introduction

Vibrations in rotorcraft are inherent, arising from the interaction between the rotors' mechanical components and the airflow on the blades. Their effects range from structural fatigue to reduced operational efficiency and even, in extreme cases, operational safety. The latter is generally caused by their effects on pilots and operators, which can include fatigue and discomfort, reduced situational awareness, task performance degradation, increased workload, and the potential reduction of flying qualities and safety caused by vibration feedthrough at the control inceptors, mediated by the pilots' biomechanics.

Phenomena arising from the interaction between the pilot biomechanics and the vehicle vibrations affecting the flying qualities are referred to under the comprehensive term of (Adverse) Rotorcraf-Pilot Couplings, or RPCs[1]. In particular, phenomena involving pilot inputs that are not control-related typically occur in the 2 Hz–8 Hz range, a frequency range that is well beyond the intentional manual control of human beings, thus only attributable to biomechanical filtering of vibratory inputs. They are often referred to as Pilot-Assisted Oscillations, or PAOs, and are the focus of the present work [1].

A typical PAO problem, often taken as a reference for its simplicity and relevance, is the vertical (or collective, in the case of helicopters) bounce. It is characterized by the feedback loop created by the interaction between the vehicle's vertical motion – controlled by the vertical component of the main rotor thrust in helicopters – and the rotation of the collective inceptor, mediated through the pilot's biomechanical response. Since the collective lever rotation ultimately controls the main rotor thrust magnitude, vertical cockpit vibrations induced by periodic variations of thrust are transferred to the pilot body, and fed through it to the collective inceptor, potentially augmenting the thrust oscillations.

The analysis of PAOs, necessary to understand and prevent their occurrence, especially in new designs, involves the modeling and testing of the relevant vehicle dynamics and of the biomechanical response of the pilot that is excited by the vehicle motion. In the case of collective bounce, the aircraft heave motion and collective flap dynamics have proven to be sufficient to accurately represent the vehicle behavior for stability analysis [2]. The input-output relationship between the vehicle accelerations and either the control device deflections or total force applied to it through the pilot's hand. It is often referred to as the BioDynamic FeedThrough, or BDFT, of the Pilot Control Device System (PCDS). Adopting the naming conventions of [3], when the output is the rotation of the collective lever, the BDFT takes the name of B2P, or BDFT to Positions.

Regarding the pilot model, research focus has been placed on simple one degree of freedom, linear models [2] and on detailed, multibody models of the human upper body [4]. The PAOs analysis is a combination of modeling and testing the so-called BioDynamic FeedThrough (BDFT) [5]. The pilot can be described from different approaches, via a physical multibody point of view, or through a more black box scheme, like in McRuer's works [6]. The latter choice is often employed to fit experimental data [7] (Cf. Figure 2).
This work represents an attempt at bridging the gap between the two model schematics: the development of several medium-complexity models of the pilot biomechanics is presented. The modeling effort has the following objectives:

- provide a clear identification of the contributions, in terms of generalized forces, that influence the B2P;
- physically represent the components of the scheme and decomposition proposed by Venrooij in [3] (Cf. Figure1);
- verify the results of Venrooij's works, considering a different application;
- develop a simplified model for control synthesis.

Figure 1 illustrates the conceptual model of the BDFT system proposed by Venrooij in [3], which maps the relationships among its various components. This diagram includes all the elements typically found in a BDFT system. Each block within the model is linked to a transfer function (denoted by H) that describes the dynamics of the respective system components. This research introduces a cohesive framework for tackling the BDFT problem, addressing the inconsistencies in definitions, nomenclature, and mathematical descriptions prevalent in previous studies. The fragmented nature of BDFT literature has hindered the comparison of results and the advancement of a comprehensive understanding of BDFT phenomena. The work in [3] makes a substantial contribution by creating a detailed framework for BDFT analysis, which includes a standardized set of definitions, nomenclature, and mathematical notations. This unified approach facilitates the study, discussion, and comprehension of BDFT and its related issues.
To best achieve the aforementioned objectives, the modeling follows an incremental path in the development of several realizations of different complexities. The elements are always rigid bodies, holonomic constraints, and linear viscoelastic elements, but their number increases. In all cases, the rigid bodies describe the motion of the arm, forearm, and collective lever; the system is always simplified as planar, its motion being confined in a vertical plane.
The adopted approaches are the following:

1. 1 Degree of Freedom (DoF): the system has a prescribed Degree of Freedom, the vertical movement of the base, and a degree of freedom associated with the rotation of the collective lever. A single rigid body is used to represent the pilot body;
2. 2 degrees of freedom, with only rigid bodies: like the 1 DoF but with the arm divided into hand and shoulder, constrained by an equivalent spring-damper system;
3. 2 degrees of freedom, with only rigid bodies: like the 1 DoF but with the arm divided into forearm and arm, hinged at the elbow. The system's kinematics is more adherent to reality;

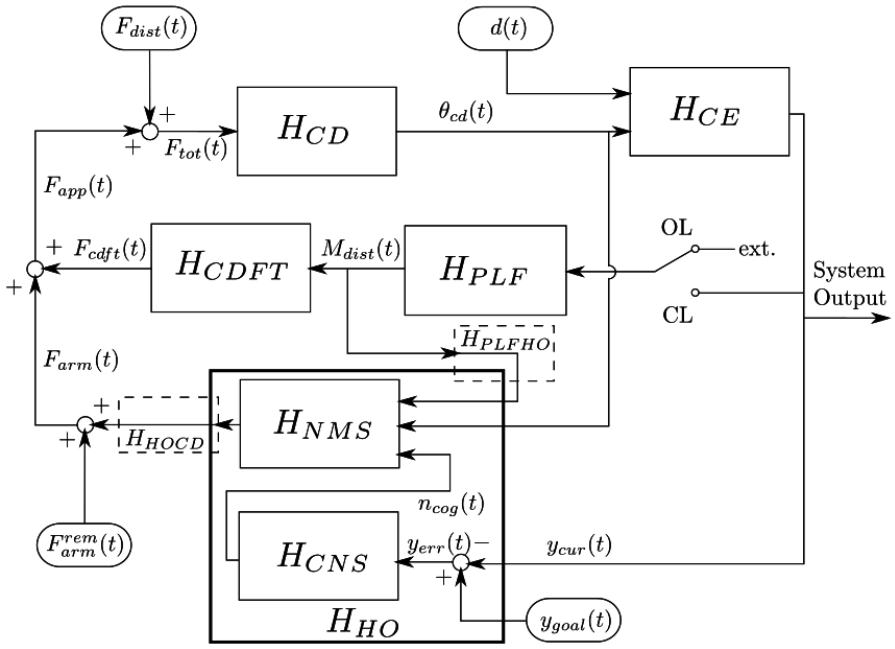

(a) Block scheme for BDFT system, overall (courtesy of Joost Venrooij)

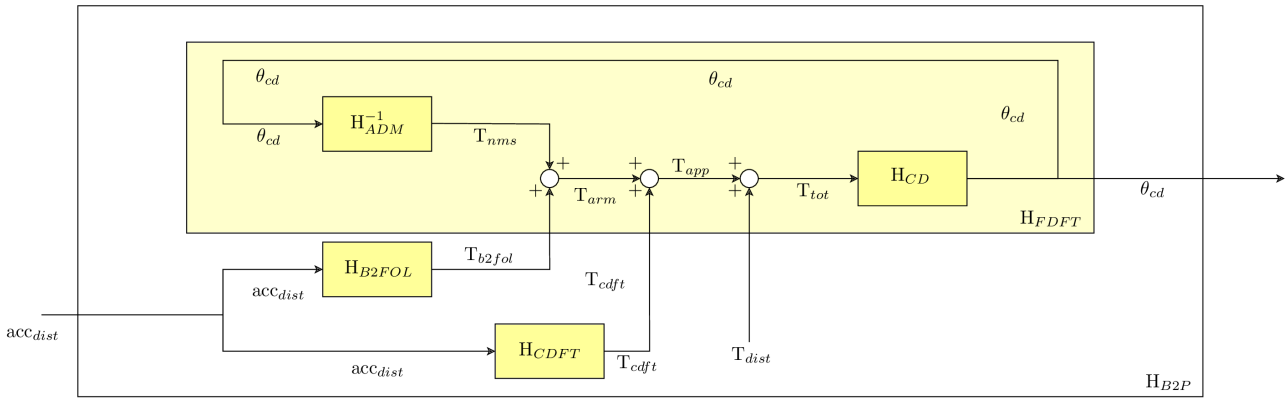

(b) Block scheme for BDFT in details

Figure 1 – Pilot-vehicle interface block decomposition (from [3])

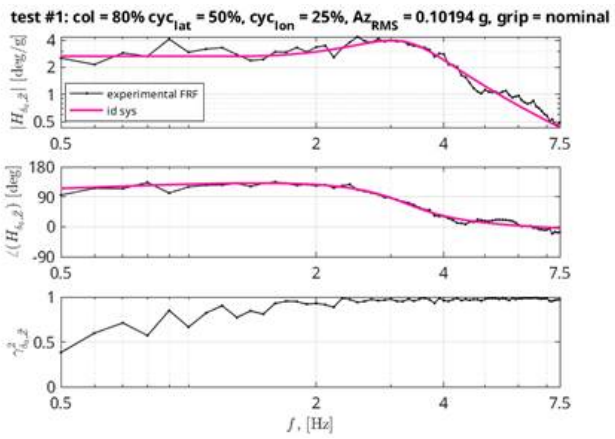

Figure 2 – BDFT fitting, given the black-box model

The goal of this investigation is to understand if it is possible to obtain simple, physics-based models for which identifying and managing the contribution of each element is easy.
The objectives are to provide a clear explanation of the physics and geometry of each contribution and how this influences the parameters that characterize the system's frequency response, in particular: the static gain, the resonance frequencies, and their corresponding damping.
This paper intends to provide these quantities in an analytically clear manner, where "clear" means the symbolic representation of the relationships that constitute the characteristic parameters of the system, allowing an informed reader to attribute meaning and significance to the expression.
Even a second-order system with two degrees of freedom involves a state-space realization matrix A of dimension 4×4, thereby immediately complicating the objective of explicitly showing the algebraic relationships that compose the expressions of the parameters.
Nonetheless, there remains the possibility of directly extrapolating the matrix expressions from the model, thereby allowing the numerical quantities to be physically parameterized. This enables the individual components of the BDFT to be obtained directly, without the need to execute ad-hoc virtual or real experiments [7].
Attributing a physical parameterization to the characterization of the system allows for the hypothesizing of good initial guesses for the measurable quantities. This is possible because the geometric relationships are maintained, unlike in [3]. Moreover, it should allow for tuning the system with a smaller set of variables compared to the parameterization of the equivalent state space model.
Another opportunity provided by this approach is the possibility to study the behavior as a function of different equilibrium points without having to rely on time-marching simulations. Additionally, it allows the formulation of an LPV (Linear Parameter-Varying) system dependent on the configuration, thus enabling this type of approach for potential control.
Alongside this objective, another fundamental issue is understanding the level of complexity required to faithfully reconstruct the phenomenon under investigation, as well as the ability to attribute physical meaning to each component. To achieve this, one can proceed in various directions, for example, by evaluating the eigenvalues of a sophisticated model as in [4] or by attempting to obtain them from experiments through an SVD decomposition of the data or their transformation into the frequency domain. This approach can be described as top-down. The approach followed in this paper is bottom-up, where a model is incrementally built to be more complex and compared with experimental or simulation data.

2. Methods and Models

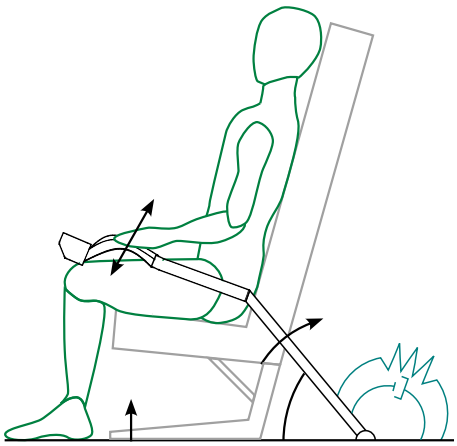

Figure 3 – Physical model of the system

To best elucidate the physical relationships governing the system and immediately formulate the equations of motion, a virtual work approach has been used rather than using a Lagrangian approach or the cardinal equations of dynamics. It is believed that this method makes the attribution of contributions more easily understandable even in this initial phase of modeling. After all, one can

imagine infinitesimal work as the quantification of the effect of force on the variation of infinitesimal displacement.

As previously presented, the modeling begins with the single-degree-of-freedom model found in [2], which is reformulated here to allow for comparison with the subsequently developed models. From this model, all explicit symbolic expressions can be derived. Briefly, the model involves a single body composed of a point mass attached to the end of a rod. This rod represents the collective control lever of the helicopter, while the point mass represents the pilot assembly, including the torso, arms, and hand. The rod is not modeled as uniform to account for the presence of the grip and the inertia properties of the control chain. The pilot's body is modeled as a spring-damper system constrained to the ground via a skid, while the collective lever rod has a rotational spring and damper applied to it to simulate the effects of the balancing spring and the friction in the control chain. The rod is hinged to the ground. The system is excited by a base acceleration.

In the second modeling approach, the pilot assembly is divided into two bodies: one mass representing part of the arm plus the hand welded to the control rod, and another mass representing the torso, shoulder, and part of the arm constrained with a vertical skid to the base, allowing movement along the direction of external acceleration. The two masses are connected via a spring-damper couple to allow the arm's flexibility to move while still maintaining relative dependence and the ability to represent and manage muscle activation. The shoulder position is maintained by another spring-damper couple, allowing the introduction of the mode associated with the torso/spinal column/seat system.

This model is considered the clearest and sufficiently complex to best capture the dynamics of the human body; for this reason, it will be extensively described in the paper. It has a total of two degrees of freedom.

The third model involves replacing the spring-damper between the two masses representing the human body with a system of two non-uniform rods, representing the forearm and arm, hinged together at the ends like an elbow joint. This system is connected at the two free ends with the shoulder mass and the hand mass via two hinges. To represent the muscles of the body, three spring-damper couples are applied: at the hinge that describes the hand, acting on the forearm and control lever, at the elbow hinge acting on the arm and forearm, and at the shoulder hinge acting on the arm, grounded via a skid constraint allowing the spring to follow the vertical movement of the shoulder.

The system has two degrees of freedom but does not allow for the explicit reading of the symbolic equation of motion. However, this model effectively incorporates all the main components of the human body involved in this phenomenon. Therefore, it was decided to complete its analysis, also to verify how this geometric complexity increment develops. This model is useful for the rapid evaluation of any nonlinearities caused by large displacements while maintaining fundamental geometric relationships.

Having a reliable model still allows for the numerical decomposition of the block diagram and the evaluation of the system's characteristic parameters without virtual experiments and ad-hoc tests. Moreover, the incremental approach leverages knowledge from the simpler model to expedite the parameter identification of this one. Finally, if this model allows for good identification, it can be utilized for more detailed parametric analyses compared to the previous model, thanks to its computational efficiency. This enables both thorough and rapid analysis.

2.1 Single DoF Model

The kinematics of this model is rather straightforward. Here, positions, velocities, and accelerations are provided in both absolute and body-fixed reference frames. Where O is the origin of the absolute reference frame $(\hat{x},\hat{y})$, $\mathbf{OP}$ is the position vector of the cyclic lever, where the equivalent pilot mass is located at its end, $\mathbf{OA}$ and $\mathbf{AP}$ are its projections onto the absolute reference frame, θ is the angle with respect to the $\hat{x}$ axis, the output of the system subject to BDFT, S is the length of the lever, η is the position relative to the length S of the center of mass of the lever. The relative system, fixed to the lever, is defined by the pair of unit vectors $(\hat{n}_S,\hat{t}_S)$, where $\hat{n}_S$ exits from the control rod and $\hat{t}_S$ is orthogonal and right-handed in the plane.

$$\mathbf{OP} = \mathbf{OA} + \mathbf{AP} \tag{1}$$

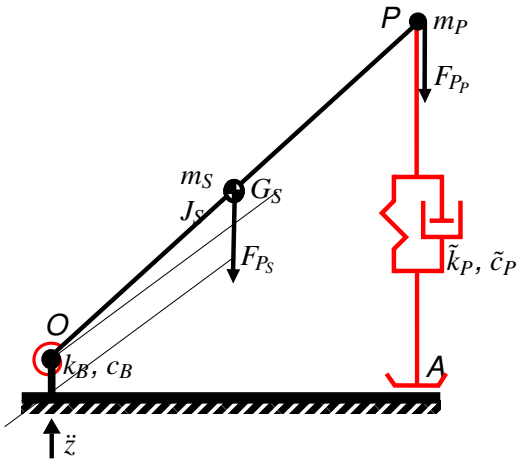

Figure 4 – Single model of the system

$$\rightarrow \begin{cases} \mathsf{OA} = S\cos\theta \\ \mathsf{AP} = S\sin\theta \end{cases} \tag{2}$$

$$\rightarrow \begin{bmatrix} \dot{\mathsf{OA}} \\ \dot{\mathsf{AP}} \end{bmatrix} = \begin{bmatrix} -S\sin\theta \\ S\cos\theta \end{bmatrix} \dot{\theta} \tag{3}$$

$$\rightarrow \begin{bmatrix} \ddot{\mathsf{OA}} \\ \ddot{\mathsf{AP}} \end{bmatrix} = \begin{bmatrix} -S\sin\theta \\ S\cos\theta \end{bmatrix} \ddot{\theta} - \begin{bmatrix} S\cos(\theta) \\ S\sin(\theta) \end{bmatrix} \dot{\theta}^2 \tag{4}$$

One can then derive the relationships for the accelerations a_{G_P}, a_P of the important points (center of gravity G_S of the lever and pilot mass P) expressed in the reference frame fixed to the bodies and the displacement θ. Similarly, the virtual displacements $\delta\mathbf{p}_{G_S}$, $\delta\mathbf{p}_P$ of the same points are defined.

$$\mathbf{a}_{G_S} = \left(-\eta S\dot{\theta}^2 + \sin(\theta)\ddot{z}\right)\hat{n}_S + \left(\eta S\ddot{\theta} + \cos(\theta)\ddot{z}\right)\hat{t}_S \tag{5}$$

$$\mathbf{a}_P = \left(-S\dot{\theta}^2 + \sin(\theta)\ddot{z}\right)\hat{n}_S + \left(S\ddot{\theta} + \cos(\theta)\ddot{z}\right)\hat{t}_S \tag{6}$$

$$\begin{aligned} \delta\mathbf{p}_{\mathsf{G}_S} &= \eta S\delta\theta\hat{t}_S \\ \delta\mathbf{p}_{\mathsf{P}} &= S\delta\theta\hat{t}_S \end{aligned} \tag{7}$$

The forces acting on the system can now be identified to define, for each one, its virtual work with respect to the virtual displacement, assemble the internal and external works, and thus obtain the equation of motion. $\mathbf{F}^{\mathsf{ine}}_{\mathsf{G}_S}, \mathbf{C}^{\mathsf{ine}}_{\mathsf{G}_S}, \mathbf{F}^{\mathsf{ine}}_{\mathsf{G}_P}$ are the inertia forces and moments of the control rod and equivalent pilot mass. $\mathbf{C}^{\mathsf{O}}_{\mathsf{v}}, \mathbf{C}^{\mathsf{O}}_{\mathsf{el}}, \mathbf{F}^{\mathsf{P}}_{\mathsf{v}}, \mathbf{F}^{\mathsf{P}}_{\mathsf{el}}, \mathbf{F}^{\mathsf{P}}_{P}$ are the elastic and viscous forces and moments of the equivalent springs and dampers acting at O on the lever and at P on the pilot mass. $\mathbf{F}^{\mathsf{G}_S}_{P}, \mathbf{C}_{\mathsf{control}}$ are the weight forces of the lever, the pilot, and the external control or disturbance torque. $c_{\mathsf{O}}, k_{\mathsf{O}}, \tilde{c}_{\mathsf{P}}, \tilde{c}_{\mathsf{P}}, \tilde{k}_{\mathsf{P}}, \tilde{k}_{\mathsf{P}}$ are the damping and elastic coefficients, while $J_S, m_P, m_{\mathsf{G}_S}, g$ are their respective masses, inertia properties, and gravitational accelerations. $\tilde{\theta}, \bar{\theta}$ are the rest lengths of the springs, related to the degree of freedom θ.

$$\begin{aligned} \mathbf{F}^{\mathsf{ine}}_{\mathsf{G}_S} &= \begin{bmatrix} m_S\eta S\dot{\theta}^2 - m_S\sin(\theta)\ddot{z} \\ -m_S\eta S\ddot{\theta} - m_S\cos(\theta)\ddot{z} \end{bmatrix}_{\hat{n}_S\hat{t}_S} \\ \mathbf{C}^{\mathsf{ine}}_{\mathsf{G}_S} &= -J_S\ddot{\theta}\hat{k} \\ \mathbf{F}^{\mathsf{ine}}_{\mathsf{G}_P} &= \begin{bmatrix} m_P S\dot{\theta}^2 - m_P\sin(\theta)\ddot{z} \\ -m_P S\ddot{\theta} - m_P\cos(\theta)\ddot{z} \end{bmatrix}_{\hat{n}_S\hat{t}_S} \end{aligned} \tag{8}$$

$$
\begin{aligned}
\mathbf{C}_{\mathsf{v}}^{\mathsf{O}} &= -c_{\mathsf{O}}\dot{\theta}\hat{k} \\
\mathbf{C}_{\mathsf{el}}^{\mathsf{O}} &= -k_{\mathsf{O}}(\theta-\tilde{\theta})\hat{k} \\
\mathbf{F}_{\mathsf{v}}^{\mathsf{P}} &= -\tilde{c}_{\mathsf{P}}(\dot{\theta}\cos\theta\sin\theta)\hat{n}_S - \tilde{c}_{\mathsf{P}}(\dot{\theta}\cos^2\theta)\hat{t}_S \\
\mathbf{F}_{\mathsf{el}}^{\mathsf{P}} &= -\tilde{k}_{\mathsf{P}}S(\sin\theta-\sin\bar{\theta})\sin\theta\hat{n}_S - \tilde{k}_{\mathsf{P}}S(\sin\theta-\sin\bar{\theta})\cos\theta\hat{t}_S \\
\mathbf{F}_{P}^{\mathsf{P}} &= -m_P g\sin\theta\hat{n}_S - m_P g\cos\theta\hat{t}_S \\
\mathbf{F}_{P}^{\mathsf{G}_S} &= -m_{\mathsf{G}_S} g\sin\theta\hat{n}_S - m_{\mathsf{G}_S} g\cos\theta\hat{t}_S \\
\mathbf{C}_{\mathsf{control}} &= C_{\mathsf{control}}(t)\hat{k}
\end{aligned}
\tag{9}
$$

From this, it is possible to derive the expression of their respective virtual works. Under the formulated assumptions, the virtual work of the internal forces is null.

$$
\begin{aligned}
\mathbf{F}_{\mathsf{G}_S}\cdot\delta\mathbf{p}_{\mathbf{S}} &= (\mathbf{F}_{\mathsf{G}_S}^{\mathsf{ine}} + \mathbf{F}_{\mathsf{P}_S})^\top \delta\mathbf{p}_{\mathbf{S}} \\
&= \begin{bmatrix} \eta S m_S\dot{\theta}^2 - m_S\sin(\theta)\ddot{z} - m_S g\sin(\theta) \\ -\eta S m_S\ddot{\theta} - m_S\cos(\theta)\ddot{z} - m_S g\cos(\theta) \end{bmatrix}^\top \begin{bmatrix} 0 \\ \eta S\delta\theta \end{bmatrix}
\end{aligned}
\tag{10}
$$

$$
\begin{aligned}
\mathbf{F}_{\mathsf{G}_P}\cdot\delta\mathbf{p}_{\mathsf{P}} &= (\mathbf{F}_{\mathsf{P}}^{\mathsf{ine}} + \mathbf{F}_{\mathsf{P}_P} + \mathbf{F}_{v}^{P} + \mathbf{F}_{\mathsf{el}}^{P})^\top \delta\mathbf{p}_{\mathsf{P}} \\
&= \begin{bmatrix} S m_P\dot{\theta}^2 - m_P\sin(\theta)\ddot{z} - m_P g\sin(\theta) - \tilde{k}_P(S\sin(\theta) - S\sin(\bar{\theta}))\sin(\theta) - \tilde{c}_P S\cos(\theta)\sin(\theta)\dot{\theta} \\ -S m_P\ddot{\theta} - m_P\cos(\theta)\ddot{z} - m_P g\cos(\theta) - \tilde{k}_P(S\sin(\theta) - S\sin(\bar{\theta}))\cos(\theta) - \tilde{c}_P S\cos^2(\theta)\dot{\theta} \end{bmatrix}^\top \begin{bmatrix} 0 \\ \delta\theta \end{bmatrix}
\end{aligned}
\tag{11}
$$

$$
\begin{aligned}
\mathbf{C}_{\theta}\cdot\delta\theta &= (\mathbf{C}_{S}^{\mathsf{ine}} + \mathbf{C}_{v}^{\mathsf{O}} + \mathbf{C}_{\mathsf{el}}^{\mathsf{O}} + \mathbf{C}_{\mathsf{control}})^\top \delta\theta \\
&= (-J_S\ddot{\theta} - c_{\mathsf{O}}\dot{\theta} + k_{\mathsf{O}}(\theta-\tilde{\theta}) + C_{\mathsf{control}}))\delta\theta
\end{aligned}
\tag{12}
$$

By summing these external virtual works and equating them to the null internal virtual work $\delta W_{ext} = \delta W_{ext} = 0$, we obtain the equation of motion:

$$
\begin{aligned}
&\rightarrow [-S^2(\eta^2 m_S + m_P) - J_S]\ddot{\theta} + (-\tilde{c}_P S^2\cos^2(\theta) - c_O)\dot{\theta} + \\
&+[-Sg(\eta m_S - m_P) + S^2\tilde{k}_P\sin(\bar{\theta})]cos(\theta) - S^2\tilde{k}_P\sin(\theta)\cos(\theta) - k_O\theta + k_O\tilde{\theta} = \\
&= S(\eta m_S + m_P)\cos(\theta)\ddot{z} - C_{cont}
\end{aligned}
\tag{13}
$$

The linearization of the equation of motion in the equilibrium condition is now demonstrated, for the block decomposition in [3]. The equilibrium condition is as follows:

$$
[-Sg(\eta m_S - m_P) + S^2\tilde{k}_P\sin(\bar{\theta})]cos(\theta) - S^2\tilde{k}_P\sin(\theta)\cos(\theta) - k_O\theta + k_O\tilde{\theta} = 0 \tag{14}
$$

The linearization:

$$
\begin{aligned}
J^\star &= \frac{\partial}{\partial\ddot{\theta}}f|_{eq} = -\eta^2 S^2 m_S - S^2 m_P - J_S \\
c^\star &= \frac{\partial}{\partial\dot{\theta}}f|_{eq} = -\tilde{c}_P S^2\cos^2(\theta_{eq}) - c_O \\
k^\star &= \frac{\partial}{\partial\theta}f|_{eq} = [Sg(\eta m_S + m_P) - S^2\tilde{k}_P\sin(\bar{\theta})]\sin(\theta_{eq}) - S^2 k_P\cos(2\theta_{eq}) - k_O
\end{aligned}
\tag{15}
$$

$$
\rightarrow J^\star\delta\ddot{\theta} + c^\star\delta\dot{\theta} + k^\star\delta\theta = S\cos(\theta_{eq})(\eta m_S + m_p)\ddot{z} - C_{cont} \tag{16}
$$

2.2 Two DoF Model - Arm Condensed

2.2.1 Kinematics

The second model involves two degrees of freedom $\mathbf{q} = [\mathrm{OD}, \theta]$ (the vertical displacement of the shoulder OD and the angular position of the collective lever θ) Three bodies with mass (torso, arm, lever) positioned at points D, B, G_S.

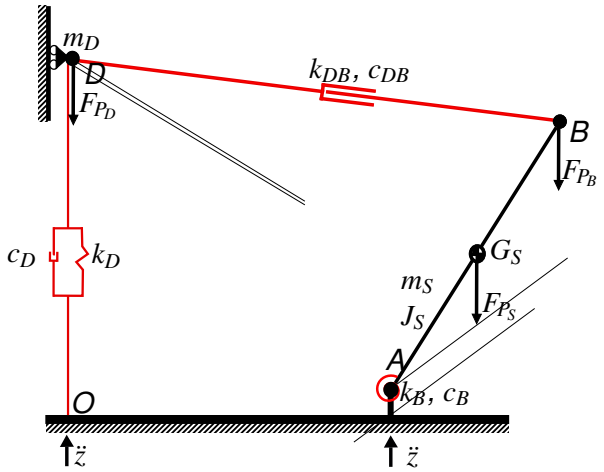

Figure 5 – Two DoF model of the system - arm condensed

AB is the vector corresponding to the control lever of length L, **AO** is the position of the pivot point of the lever relative to the projection of the shoulder onto the absolute reference system, **OD** is the vertical position of the shoulder relative to the absolute reference system, **DB** is the vector between the shoulder and the hand with origin at D and angle relative to the absolute reference system ϕ. The absolute reference system is centered at A and consists of the pair $(\hat{x},\hat{y})$, the system fixed to the lever is defined by θ, is centered at A, and consists of the pair $(\hat{n}_S,\hat{t}_S)$, the system fixed to the arm is defined by ϕ, is centered at D, and consists of the pair $(\hat{n}_{DB},\hat{t}_{DB})$. The length of the lever is S, and the relative position of the center of mass is defined by η_S.
The vector relationship between the positions is as follows:

$$\mathbf{AB} = \mathbf{AO} + \mathbf{OD} + \mathbf{DB} \tag{17}$$

It is possible to define the nonlinear relationships that link the physical variables to the minimal set of coordinates:

$$\begin{cases} \mathrm{DB}\cos(\phi) = S\cos\theta - \mathrm{AO} \\ \mathrm{DB}\sin(\phi) = S\sin\theta - \mathrm{OD} \end{cases} \tag{18}$$

From which the relationships can be explicitly derived:

$$\rightarrow \begin{cases} \mathrm{DB} = \sqrt{(S\sin\theta - \mathrm{OD})^2 + (S\cos\theta - \mathrm{AO})^2} \\ \phi = \tan^{-1}\left(\dfrac{S\sin\theta - \mathrm{OD}}{S\cos\theta - \mathrm{AO}}\right) \end{cases} \tag{19}$$

With the relationships between the positions, it is possible to define the velocities with respect to the free coordinates explicitly:

$$\begin{cases} \dot{\mathrm{DB}}\cos\phi - \mathrm{DB}\sin\phi\dot{\phi} = -S\sin\theta\dot{\theta} \\ \dot{\mathrm{DB}}\sin\phi + \mathrm{DB}\sin\phi\dot{\phi} = S\cos\theta\dot{\theta} - \dot{\mathrm{OD}} \end{cases} \tag{20}$$

$$\rightarrow \begin{cases} \dot{\mathrm{DB}} = -S\sin(\theta-\phi)\dot{\theta} - \sin\phi\dot{OD} \\ \dot{\phi} = -\dfrac{S}{\mathrm{DB}}\cos(\theta+\phi)\dot{\theta} - \dfrac{\cos\phi}{\mathrm{DB}}\dot{\mathrm{OD}} \end{cases} \tag{21}$$

From the velocity relationships, it is possible to immediately derive the virtual displacements of each relevant point with respect to the free coordinates:

$$\begin{aligned}
\delta\mathbf{p}_D &= \delta\mathrm{OD}\hat{y} \\
\delta\mathbf{p}_B &= S\delta\theta\hat{t}_S \\
\delta\mathbf{p}_{G_S} &= \eta_S S\delta\theta\hat{t}_S \\
\delta\theta &= \delta\theta\hat{k} \\
\delta\mathbf{p}_{DB} &= (-S\sin(\theta-\phi)\delta\theta - \sin\phi\,\delta\mathrm{OD})\cdot\hat{n}_{DB} = (S\delta\theta\hat{t}_S - \delta\mathrm{OD}\hat{y})\cdot\hat{n}_{DB}
\end{aligned} \tag{22}$$

2.2.2 Dynamics

The forces acting on the system are either inertial or produced by equivalent springs and dampers. The only internal forces in the system are those due to the spring-damping system of the arm $\mathbf{F}_{el}^{DB}, \mathbf{F}_{vis}^{DB}$ characterized by the coefficients k_{el}^{BD}, c_v^{BD}.
With $\mathbf{C}_{el}^{A}, \mathbf{C}_{vis}^{A}$ as the external torques introduced at A by the spring-damping system characterized by coefficients k_{el}^{A}, c_v^{A}, $\mathbf{C}_{ine}^{S}, \mathbf{F}_{ine}^{S}, \mathbf{F}_{ine_z}^{S}, \mathbf{F}_{P}^{S}$ as the inertial forces and weight of the control rod characterized by J_S, m_S, $\mathbf{F}_{ine}^{B}, \mathbf{F}_{ine_z}^{B}, \mathbf{F}_{P}^{B}$ as the inertia and weight of the mass m_B at B, $\mathbf{F}_{ine}^{D}, \mathbf{F}_{ine_z}^{D}, \mathbf{F}_{P}^{D}$ as the inertia and weight of the mass m_D at D, $\mathbf{F}_{el}^{OD}, \mathbf{F}_{vis}^{OD}$ as the external forces introduced at D by the spring-damping system present, characterized by coefficients k_{el}^{OD}, c_v^{OD}.
Below are the relationships defining these forces:

$$\begin{aligned}
&\mathbf{C}_{el}^{A} = -k_{el}^{A}(\theta-\bar{\theta})\hat{k};\quad \mathbf{C}_{vis}^{A} = -c_v^{A}\dot{\theta}\hat{k};\quad \mathbf{C}_{cont}(t) = C_{cont}\hat{k};\quad \mathbf{C}_{ine}^{S} = -J_S\ddot{\theta}\hat{k};\quad \mathbf{F}_{ine}^{S} = -\eta_S S m_S\dot{\theta}^2\hat{n}_S + \eta_S S m_S\ddot{\theta}\hat{t}_S; \\
&\mathbf{F}_{ine_z}^{S} = -m_S\ddot{z}\hat{y};\quad \mathbf{F}_{P}^{S} = -m_S g\hat{y};\quad \mathbf{F}_{el}^{DB} = -k_{el}^{DB}(DB-\bar{DB})n\hat{D}B;\quad \mathbf{F}_{vis}^{DB} = -c_v^{DB}\dot{DB}\hat{n}_{DB};\quad \mathbf{F}_{P}^{B} = -m_B g\hat{y}; \\
&\mathbf{F}_{ine_z}^{B} = -m_B\ddot{z}\hat{y};\quad \mathbf{F}_{ine}^{B} = Sm_B\dot{\theta}^2\hat{n}_S - Sm_B\ddot{\theta}\hat{t}_S;\quad \mathbf{F}_{el}^{OD} = -k_{el}^{OD}(OD-\bar{OD})\hat{y};\quad \mathbf{F}_{vis}^{OD} = -c_v^{OD}\dot{OD}\hat{y}; \\
&\mathbf{F}_{el}^{BD} = k_{el}^{DB}(DB-\bar{DB})\hat{n}_{DB};\quad \mathbf{F}_{vis}^{BD} = c_v^{DB}\dot{DB}\hat{n}_{DB};\quad \mathbf{F}_{P}^{D} = -m_D g\hat{y};\quad \mathbf{F}_{ine}^{D} = -m_D\ddot{OD}\hat{y};\quad \mathbf{F}_{ine_z}^{D} = -m_D\ddot{z}\hat{y};
\end{aligned} \tag{23}$$

From this, it is possible to express the contribution of each force to its respective virtual displacement and thus define its virtual work. All contributions of each force for its allowed virtual displacement are shown here. It is considered important to quantify and better understand the phenomenon: which degree of freedom is stimulated, which free variables are involved, and how much each term contributes relative to the others. Therefore, the following are reported:

$$\begin{aligned}
\delta W_{int}^{el_B} &= \mathbf{F}_{el}^{DB}\cdot\delta\mathbf{p}_{DB} = k_{el}^{DB}[(S\mathrm{AO}\sin\theta - S\cos\theta\mathrm{OD})\delta\theta + (OD - S\sin\theta)\delta OD] \\
\delta W_{int}^{vis_B} &= \mathbf{F}_{vis}^{DB}\cdot\delta\mathbf{p}_{DB} = c_v^{DB}[(S^2\dot{\theta} - S\cos\theta\dot{OD})\delta\theta + (\dot{OD} - S\cos\theta\dot{\theta})\delta OD] \\
\delta W_{ext}^{el_A} &= \mathbf{F}_{el}^{A}\cdot\delta\mathbf{p}_A = -k_{el}^{A}(\theta-\bar{\theta})\delta\theta \\
\delta W_{ext}^{vis_A} &= \mathbf{F}_{vis}^{A}\cdot\delta\mathbf{p}_A = -c_v^{A}\dot{\theta}\delta\theta \\
\delta W_{ext}^{cont_{G_S}} &= C_{cont}(t)\delta\theta \\
\delta W_{ext}^{P_{G_S}} &= \mathbf{F}_{P}^{G_S}\cdot\delta\mathbf{p}_{G_S} = -m_S g\eta_S S\cos\theta\delta\theta \\
\delta W_{ext}^{z_{G_S}} &= \mathbf{F}_{ine_z}^{G_S}\cdot\delta\mathbf{p}_{G_S} = -m_S\ddot{z}\eta_S S\cos\theta\delta\theta \\
\delta W_{ext}^{ine^{tr}_{G_S}} &= \mathbf{F}_{ine}^{G_S}\cdot\delta\mathbf{p}_{G_S} = -m_S\eta_S^2 S^2\ddot{\theta}\delta\theta \\
\delta W_{ext}^{ine^{rot}_{G_S}} &= \mathbf{C}_{ine}^{G_S}\cdot\delta\theta = -J_S\ddot{\theta}\delta\theta \\
\delta W_{ext}^{P_B} &= \mathbf{F}_{P}^{B}\cdot\delta p_B = -m_B g S\cos\theta\delta\theta \\
\delta W_{ext}^{z_B} &= \mathbf{F}_{z}^{B}\cdot\delta p_B = -m_B\ddot{z}S\cos\theta\delta\theta \\
\delta W_{ext}^{ine_B} &= \mathbf{F}_{ine}^{B}\cdot\delta p_B = -m_B S^2\ddot{\theta}\cos\theta\delta\theta \\
\delta W_{ext}^{P_D} &= \mathbf{F}_{P}^{D}\cdot\delta p_D = -m_D g\delta OD \\
\delta W_{ext}^{z_D} &= \mathbf{F}_{ine_z}^{D}\cdot\delta p_D = -m_D\ddot{z}\delta OD \\
\delta W_{ext}^{ine_D} &= \mathbf{F}_{ine}^{D}\cdot\delta p_D = -m_D\ddot{\mathrm{OD}}\delta OD \\
\delta W_{ext}^{el_D} &= \mathbf{F}_{el}^{D}\cdot\delta p_D = -k_{el}^{D}(\mathrm{OD}-\bar{\mathrm{OD}})\delta OD \\
\delta W_{ext}^{vis_D} &= \mathbf{F}_{vis}^{D}\cdot\delta p_D = -c_v^{D}\dot{\mathrm{OD}}\delta OD
\end{aligned} \tag{24}$$

The nonlinear equation of motion can be derived using the principle of virtual work: $\Sigma_i \delta W^i_{ext} = \Sigma_j \delta W^j_{int}$:

$$\begin{aligned}
&\rightarrow \delta\theta: \ [S^2(m_S\eta_S^2+m_B)]\ddot{\theta} + [c_A + S^2 c_{DB}]\dot{\theta} - Sc_{DB}\cos\theta\dot{\mathsf{OD}} + \\
&k_A\theta + gS(\eta_S m_S + m_B)\cos(\theta) + S\mathsf{AO}k_{DB}\sin\theta + Sk_{DB}\cos\theta\mathsf{AO}k_{DB}\sin\theta + Sk_{DB}\cos\theta\mathsf{OD} - k_A\bar{\theta} = \\
&= C_{cont}(\mathbf{q},t) - (m_S\eta_S + m_B)S\cos\theta\ddot{z} \\
&\rightarrow \delta\mathsf{OD}: \ m_D\ddot{\mathsf{OD}} + [c_D + c_{DB}]\dot{\mathsf{OD}} - Sc_{DB}\cos\theta\dot{\theta} + [k_D + k_{DB}]\mathsf{OD} - Sk_{DB}\sin\theta - k_D\bar{\mathsf{OD}} + m_D g = \\
&= -m_D\ddot{z}
\end{aligned} \tag{25}$$

At this point, it is possible to linearize around the equilibrium point defined by the equation:

$$\begin{cases}
k_A\theta_{eq} + gS(\eta_S m_S + m_B)\cos\theta_{eq} + S\mathsf{AO}k_{DB}\sin\theta_{eq} - Sk_{DB}\cos\theta_{eq}\mathsf{OD}_{eq} - k_A\bar{\theta} = 0 \\
(k_A + k_{DB})\mathsf{OD}_{eq} - Sk_{DB}\sin\theta_{eq} - k_D\bar{\mathsf{OD}} + m_D g = 0
\end{cases} \tag{26}$$

The partial derivatives of the equation of motion are defined as follows with $\mathbf{f} = [f_1, f_2]^\top$:

$$\begin{aligned}
&\frac{\partial}{\partial\ddot{\theta}}f_1 = S^2(\eta_S^2 m_S + m_B) + J_S = m_{\theta\theta}; \quad \frac{\partial}{\partial\dot{\theta}}f_1 = c_A + S^2 c_{DB} = c_{\theta\theta}; \quad \frac{\partial}{\partial\dot{\mathsf{OD}}}f_1 = -Sc_{DB}\cos\theta_{eq} = c_{\theta D}; \\
&\frac{\partial}{\partial\theta}f_1 = k_A - gS(\eta_S m_S + m_B)\sin\theta_{eq} + S\mathsf{AO}k_{DB}\cos\theta_{eq} + Sk_{DB}\mathsf{OD}_{eq}\sin\theta_{eq} = k_{\theta\theta}; \\
&\frac{\partial}{\partial\mathsf{OD}}f_1 = -Sk_{DB}\cos\theta_{eq} = k_{\theta D}; \quad \frac{\partial}{\partial\ddot{\theta}}f_2 = m_D = m_{DD}; \quad \frac{\partial}{\partial\dot{\theta}}f_2 = c_D + c_{DB} = c_{DD}; \\
&\frac{\partial}{\partial\dot{\mathsf{OD}}}f_2 = -Sc_{DB}\cos\theta_{eq} = c_{D\theta}; \quad \frac{\partial}{\partial\theta}f_2 = k_D + k_{DB} = k_{DD}; \quad \frac{\partial}{\partial\mathsf{OD}}f_2 = -Sk_{DB}\cos\theta_{eq} = k_{D\theta}
\end{aligned} \tag{27}$$

Therefore, the linear equation is:

$$\rightarrow \begin{cases}
[S^2(\eta_S^2 m_S + m_B) + J_S]\Delta\ddot{\theta} + (c_A + S^2 c_{DB})\Delta\dot{\theta} - Sc_{DB}\cos\theta_{eq}\Delta\dot{OD} + \\
+[k_A - gS(\eta_S m_S + m_B)\sin\theta_{eq} + S\mathsf{AO}k_{DB}\cos\theta_{eq} + Sk_{DB}\mathsf{OD}_{eq}\sin\theta_{eq}]\Delta\theta - Sk_{DB}\cos\theta_{eq}\Delta\mathsf{OD} = \\
= -(m_S\eta_S + m_B)S\cos\theta_{eq}\ddot{z} + C_{cont} \\
m_D\Delta\ddot{\mathsf{OD}} - Sc_{DB}\cos\theta_{eq}\Delta\dot{\theta} + (c_D + c_{DB})\Delta\dot{\mathsf{OD}} - Sk_{DB}\cos\theta_{eq}\Delta\theta + (k_D + k_{DB})\Delta\mathsf{OD} = \\
= -m_D\ddot{z}
\end{cases} \tag{28}$$

In compact form:

$$\rightarrow \begin{bmatrix} m_{\theta\theta} & 0 \\ 0 & m_{DD} \end{bmatrix}\begin{bmatrix} \Delta\ddot{\theta} \\ \Delta\ddot{\mathsf{OD}} \end{bmatrix} + \begin{bmatrix} c_{\theta\theta} & c_{\theta D} \\ c_{D\theta} & c_{DD} \end{bmatrix}\begin{bmatrix} \Delta\dot{\theta} \\ \Delta\dot{\mathsf{OD}} \end{bmatrix} + \begin{bmatrix} k_{\theta\theta} & k_{\theta D} \\ k_{D\theta} & k_{DD} \end{bmatrix}\begin{bmatrix} \Delta\theta \\ \Delta\mathsf{OD} \end{bmatrix} = \begin{bmatrix} f_{1z} \\ f_{2z} \end{bmatrix}\ddot{z} + \begin{bmatrix} C_1(\mathbf{q},t) \\ C_2 \end{bmatrix} \tag{29}$$

It is possible to define the matrices of the state-space system:

$$\begin{aligned}
&A = \begin{bmatrix} 0 & I \\ -M^{-1}K & -M^{-1}C \end{bmatrix}; \qquad B = [0,0,f_{1z},f_{2z}]^\top \\
&C = [1,0,0,0]; \qquad\qquad\qquad D = 0
\end{aligned} \tag{30}$$

From which it is possible to derive the transfer function using the classical approach with the state space realization:

$$H(s) = C(sI - A)^{-1}B + D \tag{31}$$

This leads to the definition of the standard results for two degrees of freedom mechanical system, with coupling terms:

$$H(s) = \frac{f_{1z}m_D s^2 + (c_{DD}f_{1z} - c_{\theta D}f_{2z})s + f_{1z}k_{DD} - f_{2z}k_{DD}}{m_D m_\theta s^4 + (c_{\theta\theta}m_D + c_{DD}m_\theta)s^3 + (c_{DD}c_{\theta\theta} - c_{D\theta}^2 + k_{\theta\theta}m_D + k_{DD}m_\theta)s^2 + (c_{DD}k_{\theta\theta} - 2c_{\theta D}k_{D\theta}c_{\theta\theta}k_{DD})s + k_{DD}k_{\theta\theta} - k_{D\theta}^2} \tag{32}$$

Therefore, it is possible to derive some of the system characteristics symbolically, including the static gain of the system $SG = H(0)$:

$$\begin{aligned} SG &= \frac{f_{1z}k_{DD} - f_{2z}k_{\theta D}}{k_{DD}k_{\theta\theta} - k_{d\theta}^2} \\ &= \frac{S\cos\theta_{eq}[k_{DB}m_B + (k_D + k_{DB})(m_B + \eta_S m_S)]}{S[(OD_{eq}k_{DB}g(m_B + \eta_S m_S))\sin\theta_{eq} + (AO - Sk_D B\cos\theta_{eq})k_{DB}\cos\theta_{eq}] - k_A} \end{aligned} \tag{33}$$

Although algebraically deriving the other quantities might be quite difficult, numerically it becomes straightforward, without the need to formulate ad hoc virtual experiments. In the following are reported the torques used in the Venrooij's decomposition to define the transfer functions in the blocks themselves.

$$\begin{aligned} C_{arm}\begin{bmatrix}1\\0\end{bmatrix} &= \begin{bmatrix} m_B S^2\cos\theta\ddot{\theta} + c_{DB}S^2\dot{\theta} - c_{DB}S\cos\theta\dot{OD} + m_B gS\cos\theta + k_{DB}S\mathsf{AO}\sin(\theta) - k_{DB}S\cos(\theta)\mathsf{OD} \\ m_D\ddot{\mathsf{OD}} + (c_{DB} + c_D)\dot{OD} - c_{DB}S\cos(\theta)\dot{\theta} + m_D g + k_D(OD - \bar{OD}) + k_{DB}(OD - S\sin\theta) \end{bmatrix} \\ \rightarrow C_{arm}^{lin}\begin{bmatrix}1\\0\end{bmatrix} &= \begin{bmatrix} m_B S^2 & 0 \\ 0 & m_D \end{bmatrix}\begin{bmatrix}\Delta\ddot{\theta}\\ \Delta\ddot{\mathsf{OD}}\end{bmatrix} + \begin{bmatrix} c_{DB}S^2 & -c_{DB}S\cos\theta_{eq} \\ -c_{DB}S\cos\theta_{eq} & c_{DB} + c_D \end{bmatrix}\begin{bmatrix}\Delta\dot{\theta}\\ \Delta\dot{\mathsf{OD}}\end{bmatrix} + \\ &+ \begin{bmatrix} -m_B gS\sin\theta_{eq} + k_{DB}S\mathsf{AO}\cos\theta_{eq} + k_{DB}S\sin\theta_{eq}\mathsf{OD}_{eq} & -k_{DB}S\cos\theta_{eq} \\ -k_{DB}S\cos\theta_{eq} & k_D + k_{DB} \end{bmatrix}\begin{bmatrix}\Delta\theta\\ \Delta\mathsf{OD}\end{bmatrix} \\ &= M_{arm}\Delta\ddot{\mathbf{q}} + C_{arm}\Delta\dot{\mathbf{q}} + K_{arm}\Delta\mathbf{q} \end{aligned} \tag{34}$$

$$C_{b2fol}\begin{bmatrix}1\\0\end{bmatrix} = \begin{bmatrix} m_B S\cos\theta_{eq} \\ m_D \end{bmatrix}\ddot{z} \tag{35}$$

$$\begin{aligned} C_{cd} &= (-J_S - \eta^2 S^2 m_S)\ddot{\theta} - c_O\dot{\theta} - \eta S m_S g\cos(\theta) - k_O\theta + k_O\tilde{\theta} \\ \xrightarrow[lin.]{} C_{cd}^{lin} &= (-J_S - \eta^2 S^2 m_S)\delta\ddot{\theta} - c_O\delta\dot{\theta} + (\eta S m_S g\sin(\theta)_{eq} - k_O)\delta\theta - \eta S m_S\cos(\theta_{eq})\ddot{z} + C_{cont} \end{aligned} \tag{36}$$

$$\begin{aligned} C_{cdft} &= \eta S m_S\cos(\theta)\ddot{z} \\ \xrightarrow[lin.]{} C_{cdft}^{lin} &= \eta S m_S\cos(\theta_{eq})\ddot{z} \end{aligned} \tag{37}$$

$$\begin{aligned} C_{dist}\begin{bmatrix}1\\0\end{bmatrix} &= \begin{bmatrix} S^2(\eta_S^2 m_S + m_B) + J_S & 0 \\ 0 & m_D \end{bmatrix}\begin{bmatrix}\Delta\ddot{\theta}\\ \Delta\ddot{\mathsf{OD}}\end{bmatrix} + \begin{bmatrix} (c_A + S^2 c_{DB}) & -Sc_{DB}\cos\theta_{eq} \\ -Sc_{DB}\cos\theta_{eq} & (c_D + c_{DB}) \end{bmatrix}\begin{bmatrix}\Delta\dot{\theta}\\ \Delta\dot{\mathsf{OD}}\end{bmatrix} + \\ &+ \begin{bmatrix} [k_A - gS(\eta_S m_S + m_B)\sin\theta_{eq} + S\mathsf{AO}k_{DB}\cos\theta_{eq} + Sk_{DB}\mathsf{OD}_{eq}\sin\theta_{eq}] & -Sk_{DB}\cos\theta_{eq} \\ -Sk_{DB}\cos\theta_{eq} & (k_D + k_{DB}) \end{bmatrix}\begin{bmatrix}\Delta\theta\\ \Delta\mathsf{OD}\end{bmatrix} \\ &= M_{fdft}\Delta\ddot{\mathbf{q}} + C_{fdft}\Delta\dot{\mathbf{q}} + K_{fdft}\Delta\mathbf{q} \end{aligned} \tag{38}$$

For the Control Device and the Biodynamic feedthrough to forces in open loop (B2FOL) contributions it is simple to obtain the symbolic transfer functions stated below. For the Admittance and Force disturbance feedthrough the solution is a bit more involved and it required to exploit the 32 equation with the torques definition presented in 38, 34.

$$\begin{aligned} H_{cd} &:= \frac{\theta_{cd}}{C_{tot}^{cd}} = \frac{1}{(-J_S - \eta^2 S^2 m_S)s^2 - c_O s + (\eta S m_S g\sin(\theta_{eq}) - k_O)} \\ H_{cdft} &:= \frac{C_{cdft}}{\ddot{z}} = m_S\eta_S S\cos\theta_{eq} \\ H_{bfol} &:= \frac{C_{arm}}{\ddot{z}} = m_B S\cos\theta_{eq} \\ H_{adm}^{-1} &:= \frac{C_{arm}}{\theta} = \left[(s^2 M_{arm} + sC_{arm} + K_{arm})^{-1}\begin{bmatrix}1\\0\end{bmatrix}\right]^{-1} \\ H_{fdft} &:= \frac{\theta_{cd}}{C_{dist}} = (s^2 M_{fdft} + sC_{fdft} + K_{fdft})^{-1}\begin{bmatrix}1\\0\end{bmatrix} \end{aligned} \tag{39}$$

2.3 2 DoF Model - Geometrically Correct Arm

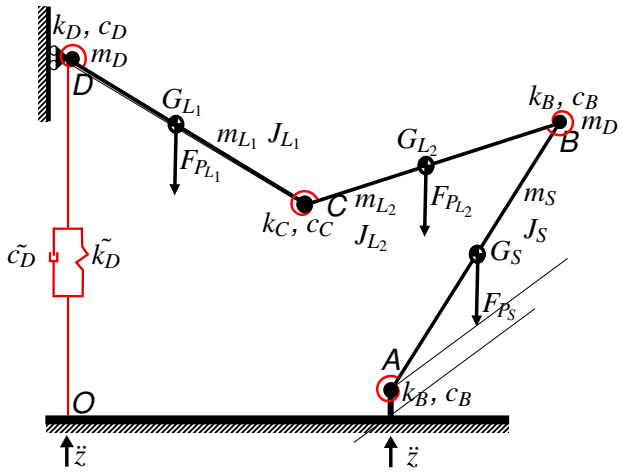

Figure 6 – 2 DoF model of the system - geometrically correct arm

Now the results of the most geometrically representative modeling are provided through only the equations of motion and the kinematic relationships; the decomposition into virtual works is not explicitly provided, although it is an important investigative tool. First, the fundamental kinematic relationships are shown:

$$Se^{i\theta(t)} = OAe^{i\pi} + OD(t)e^{i\frac{\pi}{2}} + L_1 e^{i\alpha(t)} + +L_2 e^{i\beta(t)} \tag{40}$$

Da cui:

$$\begin{cases} L_2\cos(\beta(t)) = S\cos(\theta(t)) - L_1\cos(\alpha(t)) - OA \\ L_2\sin(\beta(t)) + OD(t) = S\sin(\theta(t)) - L_1\sin(\alpha(t)) \end{cases} \tag{41}$$

Which admits an explicit solution of the form:

$$\begin{aligned} \beta(t) &= \arccos\left(\frac{Scos(\theta(t)) - L_1\cos(\alpha(t)) - OA}{L_2}\right) \\ OD(t) &= S\sin(\theta(t)) - L_1\sin(\alpha(t)) - \sqrt{L_2^2 - (S\cos(\theta(t)) - L_1\cos(\alpha(t)) - OA)^2} \end{aligned} \tag{42}$$

The equation of motion is expressed implicitly through the following parametric relationship:

$$\begin{aligned} &[(F^{\hat{n}}_{G_{L_1}} + F^{\hat{n}}_{P_{L_1}})\xi_{L_1} + (F^{\hat{n}}_{G_{L_1}} + F^{\hat{n}}_{P_{L_1}})\zeta_{L_1} + (F^{\hat{n}}_{G_{L_2}} + F^{\hat{n}}_{P_{L_2}})\xi_{L_2} + (F^{\hat{n}}_{G_{L_2}} + F^{\hat{n}}_{P_{L_2}})\zeta_{L_2} + (F^D_v + F^D_{el} + F^{ine}_D + F_{P_D})]\delta OD + \\ &[(F^{\hat{t}}_{G_{L_1}} + F^{\hat{t}}_{P_{L_1}})\eta_{L_1} + (F^{\hat{n}}_{G_{L_2}} + F^{\hat{n}}_{P_{L_2}})\mu_{L_2} + (F^{\hat{t}}_{G_{L_2}} + F^{\hat{t}}_{P_{L_2}})\eta_{L_2} + (C^{ine}_{L_1} + C^D_v + C^D_{el} + C^C_v + C^C_{el})]\delta\alpha + \\ &[(F^{\hat{t}}_{G_{L_2}} + F^{\hat{t}}_{P_{L_2}})\rho_{L_2} + (C^{ine}_S - C^C_v - C^C_{el} + C^B_v + C^B_{el})]\delta\beta + \\ &[(F^{\hat{t}}_{G_S} + F^{\hat{t}}_{P_S})\lambda_S + (C^{ine}_S + C^A_v + C^A_{el} - C^B_v - C^B_{el} + C_{cont})]\delta\theta = 0 \end{aligned} \tag{43}$$

Where the projection and transport formulas are:

$$\begin{aligned} &\xi_{L_1} = \sin(\alpha); \quad \zeta_{L_1} = \cos(\alpha); \quad \xi_{L_2} = \sin(\beta); \quad \zeta_{L_2} = \cos(\beta); \\ &\mu_{L_2} = L_1\sin(\beta - \alpha); \quad \eta_{L_2} = L_1\cos(\beta - \alpha); \quad \eta_{L_1} = \frac{L_1}{2}; \quad \rho_{L_2} = \frac{L_2}{2}; \quad \lambda_S = \frac{S}{2} \end{aligned} \tag{44}$$

The contributions due to inertial forces are reported:

$$
\begin{aligned}
&F^{\hat{n}}_{G_{L_1}} = \frac{L_1}{2} m_{L_1} \dot{\alpha}^2 - m_{L_1} \sin(\alpha) \ddot{OD} - m_{L_1} \sin(\alpha) \ddot{z}; \quad F_{P_D} = -m_D g; \quad F^{ine}_D = -m_D \ddot{OD} - m_D \ddot{z}; \quad F^{\hat{n}}_{P_{L_1}} = -m_{L_1} g \sin(\alpha) \\
&F^{\hat{n}}_{P_{L_1}} = -m_{L_1} g \cos(\alpha); \quad F^{\hat{t}}_{G_{L_1}} = -\frac{L_1}{2} m_{L_1} \ddot{\alpha} - m_{L_1} \cos(\alpha) \ddot{OD} - m_{L_1} \cos(\alpha) \ddot{z}; \quad F^{\hat{n}}_{P_{L_2}} = -m_{L_2} g \sin(\beta); \\
&F^{\hat{n}}_{G_{L_2}} = -m_{L_2} \sin(\beta) \ddot{OD} - m_{L_2} L_1 \sin(\beta - \alpha) \ddot{\alpha} + m_{L_2} L_1 \cos(\beta - \alpha) \dot{\alpha}^2 + m_{L_2} \frac{L_2}{2} \dot{\beta}^2 - m_{L_2} \sin(\beta) \ddot{z} \\
&F^{\hat{t}}_{G_{L_2}} = -m_{L_2} \cos(\beta) \ddot{OD} - m_{L_2} L_1 \cos(\beta - \alpha) \ddot{\alpha} - m_{L_2} L_1 \sin(\beta - \alpha) \dot{\alpha}^2 - m_{L_2} \frac{L_2}{2} \ddot{\beta} - m_{L_2} \cos(\alpha) \ddot{z}; \quad F^{\hat{n}}_{P_S} = -m_S g \cos(\theta); \\
&F^{\hat{n}}_{P_{L_2}} = -m_{L_2} g \cos(\beta); \quad F^{\hat{n}}_{G_S} = \frac{S}{2} m_S \dot{\theta}^2 - m_S \sin(\theta) \ddot{z}; \quad F^{\hat{n}}_{P_S} = -m_S g \sin(\theta); \quad F^{\hat{t}}_{G_S} = -\frac{S}{2} m_S \ddot{\theta} - m_S \cos(\theta) \ddot{z};
\end{aligned}
\tag{45}
$$

The other active contributions are defined as:

$$
\begin{aligned}
&C^{ine}_{G_{L_1}} = -J_{L_1} \ddot{\alpha}; \quad C^{ine}_{G_{L_2}} = -J_{L_2} \ddot{\beta}; \quad C^{ine}_{G_S} = -J_S \ddot{\theta}; \quad C^D_v = -c_D \dot{\alpha}; \quad C^D_{el} = -k_D \Delta\alpha; \\
&F^D_v = -\tilde{c}_D (\dot{OD} + \dot{z}); \quad F^D_{el} = -\tilde{k}_D (\Delta OD + z); \quad C^A_v = -c_A \dot{\theta}; \quad C^A_{el} = -k_A \Delta\theta; \quad C^B_v = -c_B (\dot{\beta} - \dot{\theta}); \\
&C^B_{el} = -k_B (\beta - \theta); \quad C^C_v = -c_C (\dot{\alpha} - \dot{\beta}); \quad C^C_{el} = -k_C (\pi + \alpha - \beta); \quad C_{cont} = C^{ext}_{cont}(t)
\end{aligned}
\tag{46}
$$

The following quantities are now defined:

$$
\begin{aligned}
\tilde{F}_{OD} &= (F^{\hat{n}}_{G_{L_1}} + F^{\hat{n}}_{P_{L_1}}) \xi_{L_1} + (F^{\hat{n}}_{G_{L_1}} + F^{\hat{n}}_{P_{L_1}}) \zeta_{L_1} + (F^{\hat{n}}_{G_{L_2}} + F^{\hat{n}}_{P_{L_2}}) \xi_{L_2} + (F^{\hat{n}}_{G_{L_2}} + F^{\hat{n}}_{P_{L_2}}) \zeta_{L_2} + (F^D_v + F^D_{el} + F^{ine}_D + F_{P_D}) \\
\tilde{C}_\alpha &= (F^{\hat{t}}_{G_{L_1}} + F^{\hat{t}}_{P_{L_1}}) \eta_{L_1} + (F^{\hat{n}}_{G_{L_2}} + F^{\hat{n}}_{P_{L_2}}) \mu_{L_2} + (F^{\hat{t}}_{G_{L_2}} + F^{\hat{t}}_{P_{L_2}}) \eta_{L_2} + (C^{ine}_{L_1} + C^D_v + C^D_{el} + C^C_v + C^C_{el} \\
\tilde{C}_\beta &= (F^{\hat{t}}_{G_{L_2}} + F^{\hat{t}}_{P_{L_2}}) \rho_{L_2} + (C^{ine}_S - C^C_v - C^C_{el} + C^B_v + C^B_{el}) \\
\tilde{C}_\theta &= (F^{\hat{t}}_{G_S} + F^{\hat{t}}_{P_S}) \lambda_S + (C^{ine}_S + C^A_v + C^A_{el} - C^B_v - C^B_{el} + C_{control})
\end{aligned}
\tag{47}
$$

Therefore:

$$
\rightarrow \tilde{F}_{OD} \delta OD + \tilde{C}_\alpha \delta\alpha + \tilde{C}_\beta \delta\beta + \tilde{C}_\theta \delta\theta = 0 \tag{48}
$$

With the relationships between virtual displacements known:

$$
\begin{aligned}
\delta\beta &= \frac{S \sin(\theta)}{L_2 \sin(\beta)} \delta\theta + \frac{L_1 \sin(\alpha)}{L_2 \sin(\beta)} \delta\alpha \\
\delta OD &= (-S \cot(\beta) \sin(\theta) + S \cos(\theta)) \delta\theta + (L_1 \cot(\beta) \sin(\alpha) - L_1 \cos(\alpha)) \delta\alpha
\end{aligned}
\tag{49}
$$

From which:

$$
\begin{aligned}
\tilde{F}_{OD}((-S \cot(\beta) sin(\theta) + S \cos(\theta)) \delta\theta + (L_1 \cot(\beta) \sin(\alpha) - L_1 \cos(\alpha)) \delta\alpha) + \\
\tilde{C}_\alpha \delta\alpha + \tilde{C}_\beta \left(\frac{S \sin(\theta)}{L_2 \sin(\beta)} \delta\theta + \frac{L_1 \sin(\alpha)}{L_2 \sin(\beta)} \delta\alpha \right) + \tilde{C}_\theta \delta\theta = 0
\end{aligned}
\tag{50}
$$

Therefore, an extremely compact formulation in terms of the unique free coordinates can be obtained, suitable for numerical implementation, of which a preliminary simulation is provided in the following image:

$$
\begin{aligned}
\left(\tilde{F}_{OD}(-S \cot(\beta) sin(\theta) + S \cos(\theta)) + \tilde{C}_\beta \left(\frac{S \sin(\theta)}{L_2 \sin(\beta)} \right) + \tilde{C}_\theta \right) \delta\theta = 0 \\
\left(\tilde{F}_{OD}((L_1 \cot(\beta) sin(\alpha) - L_1 \cos(\alpha) + \tilde{C}_\beta \left(\frac{L_1 \sin(\alpha)}{L_2 \sin(\beta)} \right) + \tilde{C}_\alpha \right) \delta\alpha = 0
\end{aligned}
\tag{51}
$$

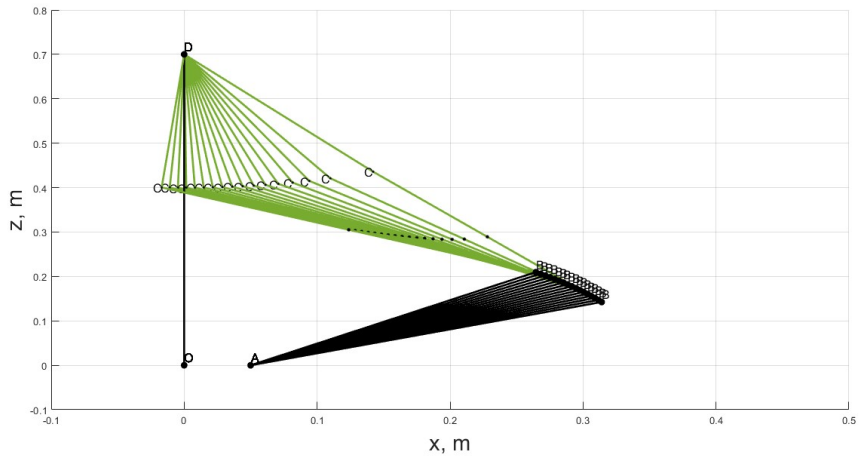

Figure 7 – Simulation for the third nonlinear model, with two degrees of freedom and geometrically correct

3. Results

The posterior results of the identification via the Greyest algorithm in Matlab are shown here. The analytical model used is the second model presented. The frequency response is simulated using the multibody model written in MBDyn and shown in the cited papers. The response is simulated at different collective angles.

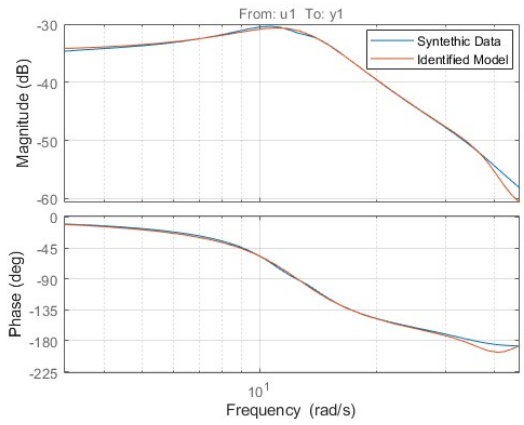

(a) 50% collective transfer function identified with educated guess

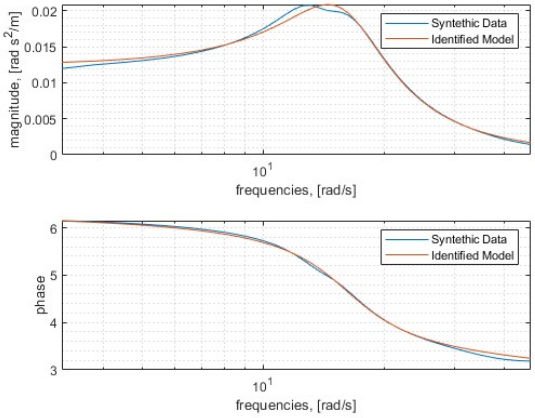

(b) 10% collective transfer function, identified with educated guess

Figure 8 – Matlab greyest results

The following transfer functions H_{BDFT} for the figures 8, 9 are found:

$$
\begin{aligned}
H_{BDFT_1} &= \frac{2.45s^2 + 36.6s + 4694}{s^4 + 24.91s^3 + 1878s^2 + 1.623 \cdot 10^4 s + 2.522 \cdot 10^5} \\
H_{BDFT_2} &= \frac{6292s^2 - 1.244 \cdot 10^8 s + 4.055 \cdot 10^{10}}{s^4 + 3.415 \cdot 10^5 s^3 + 1.247 \cdot 10^{10} s^2 + 1.267 \cdot 10^{11} s + 3.257 \cdot 10^{12}} \\
H_{BDFT_3} &= \frac{-1.165s^2 - 71.46s - 5638}{s^4 + 59.27s^3 + 2552s^2 + 3.059 \cdot 10^4 s + 4.646 \cdot 10^5}
\end{aligned}
\tag{52}
$$

The first two transfer functions exhibit a similarity of 95.4% and 95.2%. It is easy to notice from the numerical values of its matrices that the second identification provides a system with a pair of negative real roots without an imaginary part.

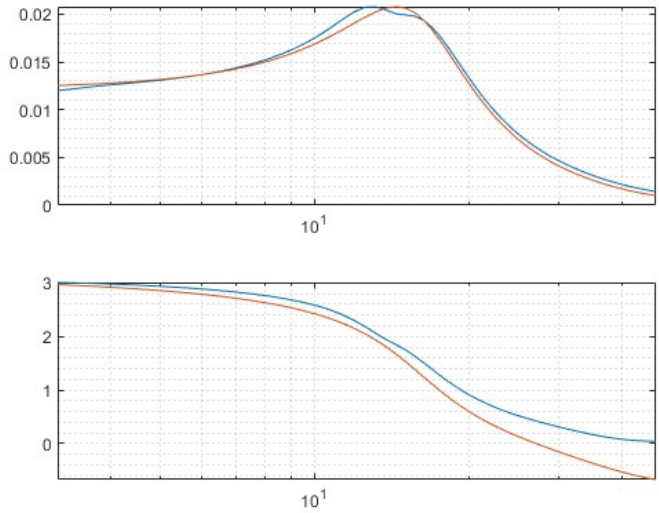

Figure 9 – Transfer function with explicit parameters identification for 10% collective

The identified values of the physical parameters, obtained without the use of Matlab's *greyest* function, for the system with the collective set at 10 degrees are presented in Figure 9. The values are identified only for the non-measurable quantities of the biomechanics of the human body: $c_{DB}, c_D, k_{DB}, k_D, m_B, m_D$ to represent the equivalent viscosity, elasticity, and mass of the torso and arm.

$$\begin{aligned} c_{DB} &= 27.986 \;\; kg/s^2 & k_{DB} &= 1.3748 \times 10^4 \;\; kg/s & m_B &= 2.9295 \;\; kg \\ c_D &= 2.2614 \times 10^3 \;\; kg/s^2 & k_D &= 6.4431 \times 10^4 \;\; kg/s & m_D &= 41.366 \;\; kg \end{aligned} \tag{53}$$

The values not identified, considered directly measurable, are the equilibrium conditions and the characteristics of the collective control stick system:

$$\begin{aligned} \theta_{eq} &= 0.3321318 \;\; rad & \mathrm{OD}_{eq} &= 0.596344 \;\; m & J_S &= 0.93 \;\; kg \times m^2 \\ m_S &= 9.94 \;\; kg & S &= 0.35148 \;\; m & \eta_S &= 0.174 \\ \mathrm{AO} &= -0.077 \;\; m & c_A &= 1.76 \;\; kg/s & k_A &= 11. \;\; kg/s^2 \end{aligned} \tag{54}$$

The state-space matrices A and B are as follows:

$$\mathrm{A} = 10^3 \begin{bmatrix} 0 & 0 & 0.001 & 0 \\ 0 & 0 & 0 & 0.001 \\ -0.4467 & 3.4371 & -0.0039 & 0.006996 \\ 0.11047 & -1.88993 & 0.000225 & -0.0553 \end{bmatrix}; \quad \mathrm{B} = \begin{bmatrix} 0 \\ 0 \\ -1.1648 \\ -1 \end{bmatrix}; \tag{55}$$

It is considered necessary to further develop methods for identification to avoid identifying false positives, as well as to make the identification of physical parameters more automatic and rapid.
Furthermore, numerical relationships for the remaining relations defining the decomposition of [3] are shown, they are referred to the second model, following equation 39.

$$\begin{aligned} H_{nms}^{-1} &= \frac{0.82736s^2 + 4.579 \times 10^2 s + 1.5636 \times 10^4}{2.9941s^4 + 1.9431 \times 10^2 s^3 + 1.2115 \times 10^4 s^2 + 3.0774 \times 10^5 s + 5.0694 \times 10^6} \\ H_{fdft} &= \frac{6.5548s^2 + 3.6278 \times 10^2 s + 1.2388 \times 10^4}{8.7718s^4 + 5.1635 \times 10^2 s^3 + 2.2234 \times 10^4 s^2 + 2.6654 \times 10^5 s + 4.4076 \times 10^6} \end{aligned} \tag{56}$$

Now, symbolic relationships are explicitly presented for the first model.

$$\begin{aligned} C_{tot} =& [-J_S - S^2(\eta^2 m_S + m_P)]\ddot{\theta} + (-c_O - \tilde{c}_P S^2\cos^2(\theta))\dot{\theta} + \\ &+ [-Sg(\eta m_S + m_P) - S^2\tilde{k}_P\sin(\theta)]\cos(\theta) - S^2 k_P\sin(\theta)\cos(\theta) - k_O\theta - k_O\tilde{\theta} + \\ &- S(\eta m_S + m_P)\cos(\theta)\ddot{z} + C_{cont} \\ \underset{lin.}{\longrightarrow} C_{tot}^{lin} =& [-J_S - S^2(\eta^2 m_S + m_P)]\delta\ddot{\theta} + (-c_O - \tilde{c}_P S^2\cos^2(\theta_{eq}))\delta\dot{\theta} + \\ &+ [Sg(\eta m_S + m_P) + S^2\tilde{k}_P\sin(\bar{\theta})]\sin(\theta_{eq}) - S^2\tilde{k}_P\cos(2\theta_{eq}) - k_O]\delta\theta + \\ &- S(\eta m_S + m_P)\cos(\theta_{eq})\ddot{z} + C_{cont} \end{aligned} \tag{57}$$

$$\begin{aligned} F_{arm} &= -Sm_P\ddot{\theta} - \tilde{c}_P S\cos^{(}\theta)\dot{\theta} + (-m_P g - S\tilde{k}_P\sin(\bar{\theta}))\cos(\theta) - S\tilde{k}_P\sin(\theta)\cos(\theta) - m_{P\cos(\theta)}\ddot{z} \\ \underset{lin.}{\longrightarrow} F_{arm}^{lin} &= -Sm_P\delta\ddot{\theta} - \tilde{c}_P S\cos^2(\theta_{eq})\delta\dot{\theta} + [(m_P g + S\tilde{k}_P\sin(\bar{\theta}))\sin(\theta_{eq}) - S\tilde{k}_P\cos(2\theta_{eq})]\delta\theta - m_P\cos(\theta_{eq})\ddot{z} \end{aligned} \tag{58}$$

$$\begin{aligned} F_{nms} &= -Sm_P\ddot{\theta} - \tilde{c}_P S\cos^{(}\theta)\dot{\theta} + (-m_P g - S\tilde{k}_P\sin(\bar{\theta}))\cos(\theta) - S\tilde{k}_P\sin(\theta)\cos(\theta) \\ \underset{lin.}{\longrightarrow} F_{nms}^{lin} &= -Sm_P\delta\ddot{\theta} - \tilde{c}_P S\cos^2(\theta_{eq})\delta\dot{\theta} + [(m_P g + S\tilde{k}_P\sin(\bar{\theta}))\sin(\theta_{eq}) - S\tilde{k}_P\cos(2\theta_{eq})]\delta\theta \end{aligned} \tag{59}$$

$$\begin{aligned} F_{b2fol} &= -m_P\cos(\theta)\ddot{z} \\ \underset{lin.}{\longrightarrow} F_{b2fol}^{lin} &= -m_P\cos(\theta_{eq})\ddot{z} \end{aligned} \tag{60}$$

$$\begin{aligned} C_{cd} &= (-J_S - \eta^2 S^2 m_S)\ddot{\theta} - c_O\dot{\theta} - \eta S m_S g\cos(\theta) - k_O\theta + k_O\tilde{\theta} \\ \underset{lin.}{\longrightarrow} C_{cd}^{lin} &= (-J_S - \eta^2 S^2 m_S)\delta\ddot{\theta} - c_O\delta\dot{\theta} + (\eta S m_S g\sin(\theta)_{eq} - k_O)\delta\theta \end{aligned} \tag{61}$$

$$\begin{aligned} C_{cdft} &= \eta S m_S\cos(\theta)\ddot{z} \\ \underset{lin.}{\longrightarrow} C_{cdft}^{lin} &= \eta S m_S\cos(\theta_{eq})\ddot{z} \end{aligned} \tag{62}$$

$$C_{dist} = C_{cont} \tag{63}$$

Therefore, it is possible to obtain the transfer functions around the equilibrium point. Please refer to the chapter on the first modeling for conventions and nomenclature.

$$\begin{aligned} H_{CD} &:= \frac{\theta_{cd}}{C_{tot}^{cd}} = \frac{1}{(-J_S - \eta^2 S^2 m_S)s^2 - c_O s + (\eta S m_S g\sin(\theta_{eq}) - k_O)} \\ H_{cdft} &:= \frac{C_{cdft}}{\ddot{z}} = \eta S m_S\cos(\theta_{eq}) \\ H_{b2fol} &:= \frac{C_{arm}}{\ddot{z}} = -Sm_P\cos(\theta_{eq}) \\ H_{adm}^{-1} &:= \frac{C_{arm}}{\theta} = -S^2 m_P s^2 - S^2\tilde{c}_P\cos(\theta_{eq})s + [S(m_P g + S\tilde{k}\sin(\theta_{eq})) - S^2\tilde{k}_P\cos(2\theta_{eq})] \\ H_{fdft} &:= \frac{\theta_{cd}}{C_{dist}} = \frac{1}{J^\star s^2 + c^\star s + k^\star} \end{aligned} \tag{64}$$

3.1 Conclusions

In this work, we have endeavored to provide detailed explanations and relationships leading to the definition of the models, considering it extremely important to enable future researchers or teams to reuse this exposition.

The presented models provide an excellent approximation of the multibody models developed by [4]. The number of parameters is reduced to 9 in its implicit form or 6 in its explicit nonlinear form for the simplest two-degree-of-freedom model.

The increasing complexity approach allows for a gradual analysis of the phenomenon in its various aspects, gradually improving the predictive capacity of the models.

Symbolically and numerically, the components of a possible block decomposition of the phenomenon have been presented. This allows for leveraging the results obtained in the literature that have different approaches, not based on the first principles of mechanics.
This work on reduced and simplified models continues by first identifying the best method to identify the parameters with the present nonlinear relationships. Secondly, it analyzes the nonlinearities described by the models, attempting to evaluate how faithful they remain to the results and, in this case, determining what contributes the most and how much these nonlinearities affect the behavior of the phenomenon. The nonlinearities may arise from the large displacements that are sometimes necessary for helicopter control.
Furthermore, there is the intention to validate the model directly using experimental data from the FRAME Sim laboratory at the Politecnico di Milano, or from flight tests, despite the somewhat complicated data collection process.
These validated models, using both synthetic and experimental data, will be employed for parametric analysis of system components where there is an interest in modifying the design of certain elements and evaluating their effects. Furthermore, it will be intriguing to understand how variations in biomechanical parameters alter the system response and how to manage the associated uncertainty. Integrating these models into those describing the overall and detailed dynamics of the helicopter will be interesting, allowing for coupling analysis.
Lastly, these models will be used to begin studying the feasibility of applying robust and LPV (Linear Parameter-Varying) control to the phenomenon, leveraging the computational speed of the model.
In summary, the work presented lays a strong foundation for further exploration and development in helicopter control system dynamics, offering a robust platform for both theoretical and practical advancements in the field.

4. Contact Author Email Address

The contact author's email address: tommaso.aresi@polimi.it

5. Copyright Statement

References

[1] Marilena D. Pavel, Michael Jump, Binh Dang-Vu, Pierangelo Masarati, Massimo Gennaretti, Achim Ionita, Larisa Zaichik, Hafid Smaili, Giuseppe Quaranta, Deniz Yilmaz, Michael Jones, Jacopo Serafini, and Jacek Malecki. Adverse rotorcraft pilot couplings — past, present and future challenges. *Progress in Aerospace Sciences*, 62:1–51, October 2013. doi:10.1016/j.paerosci.2013.04.003.

[2] Vincenzo Muscarello, Giuseppe Quaranta, and Pierangelo Masarati. The role of rotor coning in helicopter proneness to collective bounce. *Aerospace Science and Technology*, 36:103–113, July 2014. doi:10.1016/j.ast.2014.04.006.

[3] J. Venrooij, D. A. Abbink, M. Mulder, M. M. van Paassen, M. Mulder, F. C. T. d. van Helm, and H. H. Bulthoff. A biodynamic feedthrough model based on neuromuscular principles. *IEEE Transactions on Cybernetics*, PP(99):1–1, 2013. doi:10.1109/TCYB.2013.2280028.

[4] Andrea Zanoni, Alessandro Cocco, and Pierangelo Masarati. Multibody dynamics analysis of the human upper body for rotorcraft–pilot interaction. *Nonlinear Dynamics*, 102(3):1517–1539, 2020. doi:10.1007/s11071-020-06005-7.

[5] Joost Venrooij. *Measuring, modeling and mitigating biodynamic feedthrough*. PhD thesis, Technical University of Delft, 2014.

[6] D. T. McRuer. *Aviation Safety and Pilot Control: Understanding and Preventing Unfavourable Pilot-Vehicle Interactions*. Washington DC: National Research Council, National Academy Press, 1997.

[7] Andrea Zanoni Davide Marchesoli, Carmen Talamo, Pierangelo Masarati, Francesca Colombo, Sarah Kemp, and Ermanno Fosco. Experimental test-bed for the identification of biodynamic feedthrough of helicopter-pilot systems. In *48th European Rotorcraft Forum*, Winterthur, Switzerland, Sept 6–8 2022.